Proceedings of CONF-APMM 2025 Symposium: Multi-Qubit Quantum Communication for Image Transmission over Error Prone Channels
DOI: 10.54254/2753-8818/2025.GL26091

An Image Transmission System Based on Adaptive Polar Codes

Jiayang Bi

School of Electronic and Information Engineering, Hebei University of Technology, Tianjin, China
15931809510@163.com

Abstract. Leveraging the advantages of polar codes—namely their low encoding and decoding complexity and excellent bit error performance—this paper proposes a complete image transmission system based on adaptive polar codes to enhance image quality under varying channel conditions in Gaussian channels. By designing a rate lookup table tailored to specific channel conditions, the system can autonomously select coding rate parameters according to channel state information for efficient encoding and decoding. Furthermore, a comprehensive system performance evaluation framework is established using metrics such as bit error rate (BER), peak signal-to-noise ratio (PSNR), and structural similarity index (SSIM). Simulation results demonstrate that, compared with conventional digital transmission schemes based on polar codes, the proposed system achieves superior performance.

Keywords: Adaptive Polar Codes, Image Transmission, Bit Error Rate, Peak Signal-to-noise Ratio, Structural Similarity Index

1. Introduction

The rapid development of information technology has propelled image transmission technology into multiple critical domains, where modern communication systems impose dual demands for high-speed transmission and fidelity preservation under complex channel conditions [1]. However, the inherent imperfections and interference of practical channels can degrade image quality or even cause transmission failure [2]. In wireless communications, issues such as multipath effects and Doppler shifts further increase the likelihood of failure [3]. Efficient transmission under limited bandwidth has thus become a critical challenge in the communications field [4].

Channel coding techniques are essential for ensuring the reliability of image transmission, enabling error correction and recovery through the addition of redundant information [5]. While conventional methods exhibit various limitations, polar codes—being the first class of error-correcting codes proven to achieve channel capacity—offer superior performance and have been adopted as the standard for control channel coding in certain 5G scenarios. Their application in image transmission has accordingly drawn considerable attention [6]. Relevant studies have examined the influence of different channel types [7], decoding algorithm optimizations [8], and integrations with other technologies [9]. However, these works generally overlook the time-varying

© 2026 The Authors. This is an open access article distributed under the terms of the Creative Commons Attribution License 4.0 (https://creativecommons.org/licenses/by/4.0/).

DOI: 10.54254/2753-8818/2025.GL26091

nature of channels. Traditional schemes suffer from the so-called "cliff effect," where system performance reaches a bottleneck once the channel quality exceeds a certain threshold [10].

To address these limitations, this paper proposes an adaptive polar-coded image transmission system based on polar code theory and channel quality estimation. Prior to transmission, the system adaptively determines the coding rate using a pre-designed rate lookup table, thereby ensuring accurate image reception.

2. Principle of adaptive polar codes

Polar coding is based on the theory of channel polarization. It involves combining N independent binary discrete memoryless channels (BDMCs) into a joint channel, followed by a channel-splitting operation that results in the phenomenon of channel polarization. After splitting, a portion of the resulting sub-channels have capacities close to 0 (completely noisy channels), while others approach a capacity of 1 (noise-free channels). However, the total channel capacity remains unchanged, and transmitting data through the noise-free channels allows the system to approach the Shannon limit.

An (N,M) polar encoder is used to transmit source bits over the communication channel, where the code rate is R=M/N, with M denoting the number of information bits and N the codeword length. The synthesized channel is thus divided into M reliable sub-channels and N−M noisy sub-channels. Information bits are assigned to the most reliable sub-channels, while frozen bits are transmitted over the noisy ones. Since code construction based on specific channel conditions can introduce delay, the 5G standardization body has proposed a universal reliability sequence of length 1024—ranked by sub-channel reliability—which enables the construction of polar codes with lengths up to 1024 or shorter. This paper adopts that sequence for system design. The adaptive design of the proposed system maintains a fixed codeword length N, while varying the number of information bits according to the channel state, thereby achieving a variable code rate. Finally, the encoded codewords are modulated and transmitted through the communication channel. At the decoder, the system employs a serial cancellation list (SCL) decoding algorithm enhanced with cyclic redundancy check (CRC) to reconstruct the transmitted image.

3. System design

3.1. Overall architecture

In the block diagram of the adaptive polar-coded image transmission system proposed in this paper, the transmitter first reads a single-channel grayscale image, which is mapped into a two-dimensional matrix (with each pixel represented by 8 bits). After binary mapping, the image is converted into a 0–1 bitstream and divided into blocks for separate transmission. Channel-adaptive encoding and QPSK modulation are then performed. The system acquires the signal-to-noise ratio (SNR) information of the channel to adjust the coding rate dynamically, thereby adapting to complex channel conditions. Finally, the encoded signal is transmitted through a Gaussian channel, where additive white Gaussian noise (AWGN) of varying intensity is introduced to simulate real-world environments.

At the receiver side, inverse operations are carried out: demodulation and decoding are performed to obtain the binary image matrix, which is then reconstructed into a two-dimensional image. Unlike conventional systems, the proposed system employs an adaptive channel coding scheme. Before transmission, it determines the optimal coding rate based on current channel conditions and a predefined rate lookup table, enabling efficient image transmission.

DOI: 10.54254/2753-8818/2025.GL26091

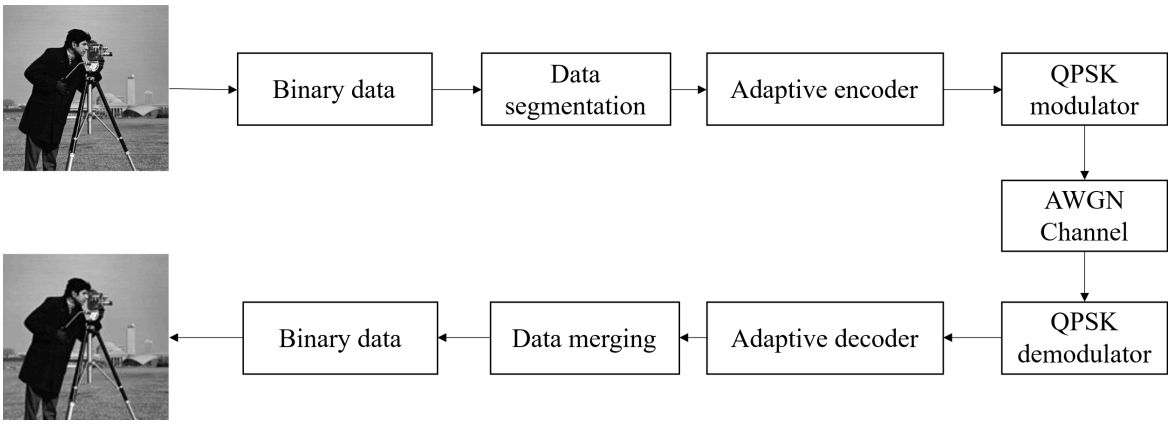


Figure 1. Block diagram of the image transmission system based on adaptive coding

3.2. Lookup table design

This system determines the optimal transmission rate based on a predefined rate lookup table. When the bit error rates are similar, a higher coding rate is selected to improve efficiency; under low signal-to-noise ratio (SNR) conditions, a lower coding rate is used to preserve image quality. Therefore, we first transmitted various test images under different SNR conditions using different coding rates and recorded the bit error rates before and after transmission. As shown in Figure 2, by analyzing the bit error rate distribution of several benchmark test images under varying channel conditions, we designed the rate lookup table presented below.

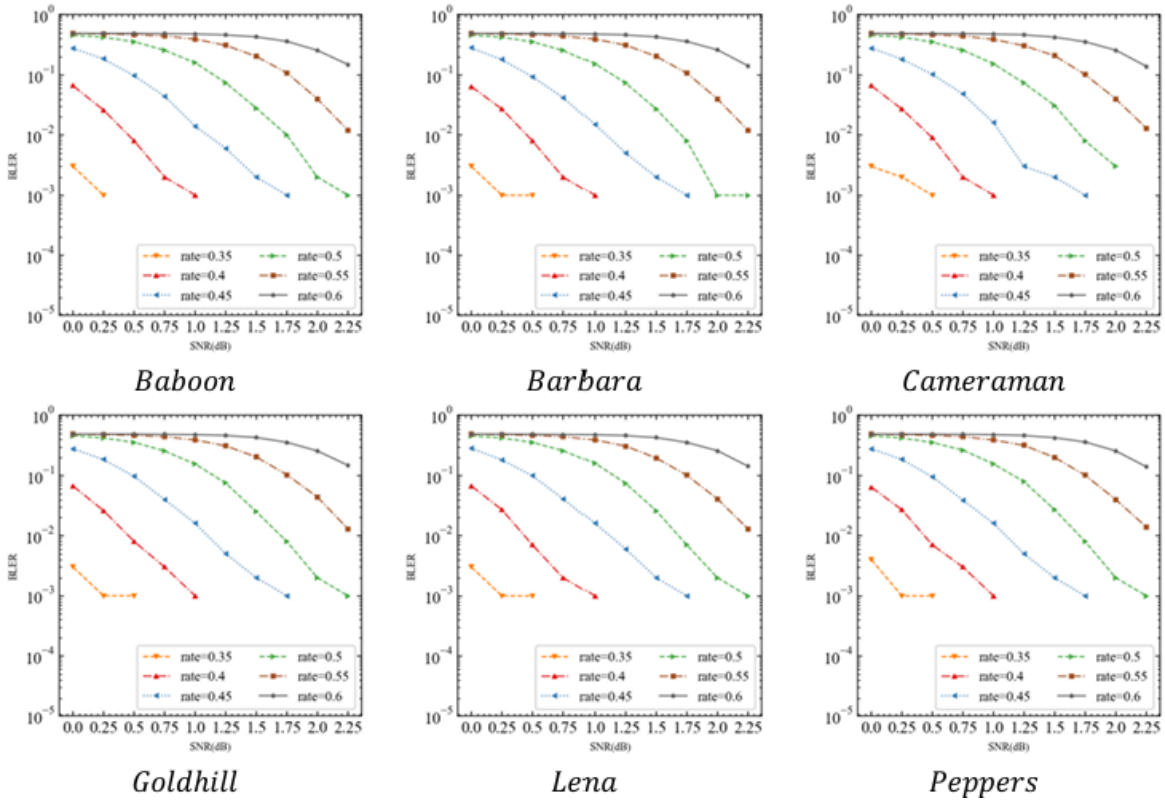


Figure 2. Bit error rate analysis of various images under different coding rates and channel conditions

DOI: 10.54254/2753-8818/2025.GL26091

Table 1. Coding rate lookup table for awgn channels

SNR(dB)	0<SNR<1.5	1.5<SNR<1.75	1.75<SNR<2.0	2.0<SNR<2.25
Transmission Code Rate	0.4	0.45	0.5	0.55

4. Simulation results

4.1. Experimental setup

4.1.1. Dataset description

The system is tested using standard grayscale images with a resolution of 512 × 512 pixels, as shown in the figure below. These images are widely used in the field of image processing and contain rich detail, enabling a comprehensive evaluation of the image transmission system's performance in preserving fine details, handling smooth regions, and processing complex textures and edges. They serve as a basis for assessing the system's image reconstruction capability.

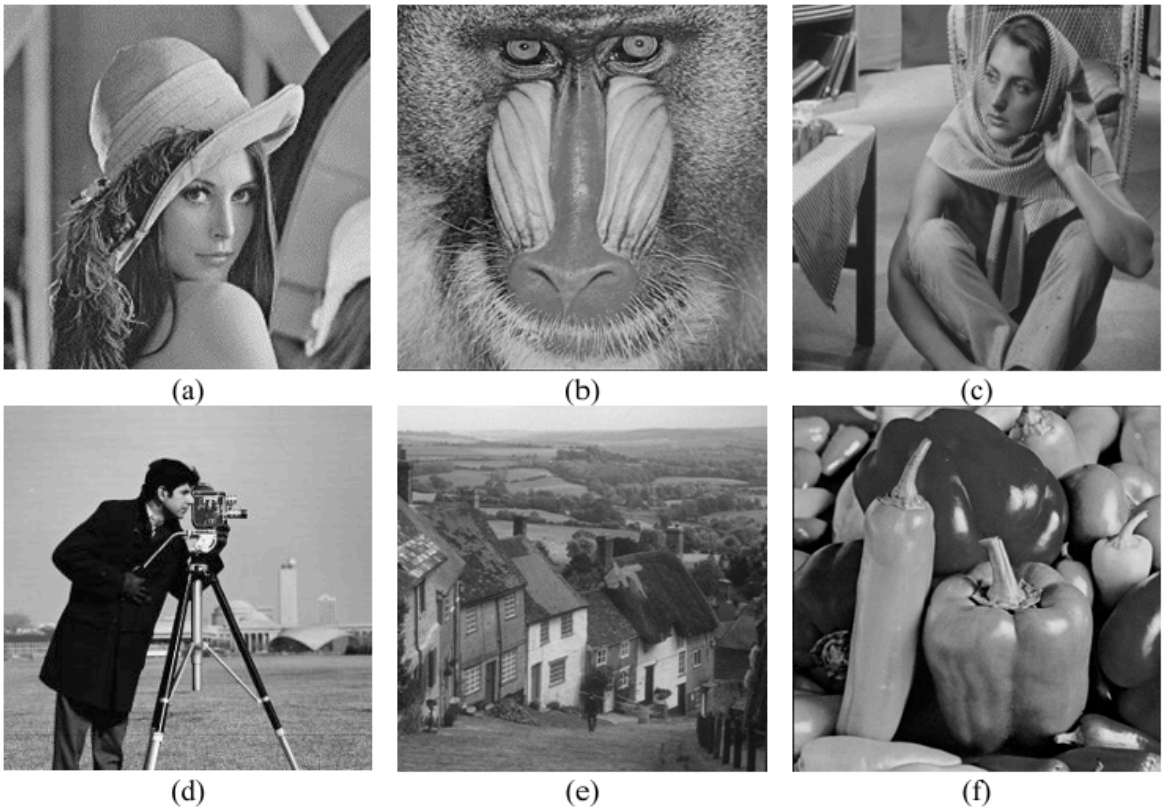


Figure 3. Benchmark test dataset: (a) Baboon; (b) Barbara; (c) Cameraman; (d) Goldhill; (e) Lena; (f) Peppers

4.1.2. Evaluation metrics

To comprehensively validate the effectiveness of the proposed system, multiple evaluation metrics are selected, with their calculation formulas provided below. Among these metrics, the bit error rate (BER) primarily measures the accuracy of the digital signal during transmission and represents the proportion of erroneous bits in the total transmitted bits. The peak signal-to-noise ratio (PSNR)

DOI: 10.54254/2753-8818/2025.GL26091

reflects image quality by measuring the mean squared error (MSE) between the original and reconstructed images. Based on the concept of signal and noise, PSNR converts image quality assessment into a ratio between the signal (original image) and noise (distortion). The structural similarity index (SSIM) is an image quality assessment metric grounded in the human visual system (HVS) perception model. It evaluates the similarity between two images comprehensively from luminance, contrast, and structural aspects. Compared with traditional pixel-error-based metrics, SSIM more accurately reflects human subjective perception of image quality [11].

$$BER = \frac{Number\ of\ Received\ Error\ Bits}{Total\ Number\ of\ Transmitted\ Bits} \tag{1}$$

$$PSNR = 10log_{10}\left(\frac{255^2}{MSE}\right) \tag{2}$$

Here, $\mathrm{MSE}=\frac{1}{\mathrm{A}\times\mathrm{A}}\sum_{\mathrm{a}=1}^{\mathrm{A}}\sum_{\mathrm{b}=1}^{\mathrm{A}}||\mathrm{I(a,\ b)\text{-}R(a,\ b)}||^2$, where $\mathrm{I(a,\ b)}$ represents the original pixel value in an image of resolution $\mathrm{A}\times\mathrm{A}$, and $\mathrm{R(a,\ b)}$ denotes the corresponding reconstructed pixel value at the same position.

$$SSIM\left(I,\ R\right) = \frac{(2\mu_I\mu_R+C_1)(2\sigma_{IR}+C_2)}{(\mu_I^2+\mu_R^2+C_1)(\sigma_I^2+\sigma_R^2+C_2)} \tag{3}$$

Here, μ_I, μ_R, σ_I, σ_R, and σ_{IR} denote the means, standard deviations, and cross-covariance of the original and reconstructed images, respectively. To avoid division by zero when $\mu_I^2+\mu_R^2$ or $\sigma_I^2+\sigma_R^2$ approach zero, constants C_1 and C_2 are introduced. For grayscale images, the default values of these constants are $C_1=(0.01\times255)^2$ and $C_2=(0.03\times255)^2$. The SSIM value ranges between 0 and 1; the closer it is to 1, the higher the perceived similarity between the original and reconstructed images.

4.1.3. Simulation details

Based on the communication system block diagram, the detailed settings for the entire experimental simulation are presented in the table below. During each simulation, multiple trials are conducted to minimize the impact of random fluctuations and ensure the most objective results.

Table 2. Summary of simulation settings

Parameter	Value
Image Size	512×512 pixels
Coding Length (N)	1024
Modulation Scheme	QPSK
Cyclic Redundancy Bits	24
Channel Model (SNR)	0:0.25:2.25(AWGN)
Adaptive Polar Code Rates	{0.4,0.5,0.6}(AWGN)
Evaluation Metrics	BER ; $PSNR$; $SSIM$

DOI: 10.54254/2753-8818/2025.GL26091

4.2. Results analysis

Figure 4 illustrates the performance comparison between the traditional scheme and the proposed system under different signal-to-noise ratio (SNR) conditions. Regarding bit error rate (BER), in low-SNR Gaussian channel environments, traditional image transmission systems use polar codes with fixed parameters for channel coding, resulting in peak signal-to-noise ratio (PSNR) closely tied to channel quality. In contrast, the adaptive polar-coded image transmission system dynamically adjusts coding parameters based on channel state information, thereby enhancing error correction capability and significantly improving PSNR under low-SNR channel conditions. In terms of the structural similarity index (SSIM), at low SNR levels (0 dB to 1 dB), the traditional system yields SSIM values below 0.2, indicating considerable distortion in the reconstructed images, with degraded detail and clarity. The adaptive polar-coded system achieves SSIM values above 0.8, showing that the reconstructed images are much more similar to the originals, with better preservation of details and clarity. Consequently, the image quality is markedly superior to that of the traditional system.

Comparing with traditional image transmission systems, the adaptive polar-coded image transmission system demonstrates clear advantages in PSNR, SSIM, and other performance metrics. The adaptive mechanism of polar codes enables better accommodation of varying channel conditions, effectively reducing BER and improving both image transmission quality and transmission rate, thus providing stronger assurance for reliable and efficient image transmission.

Table 3 compares the objective image quality of Lena, Baboon, Bridge, Goldhill, and Barbara images under different channel conditions by presenting their average PSNR and SSIM values in two transmission scenarios. Observing the results, it can be concluded that across all tested channel qualities, the proposed system outperforms the fixed-rate transmission scheme by approximately 20 dB in average PSNR and 0.4 in SSIM.

DOI: 10.54254/2753-8818/2025.GL26091

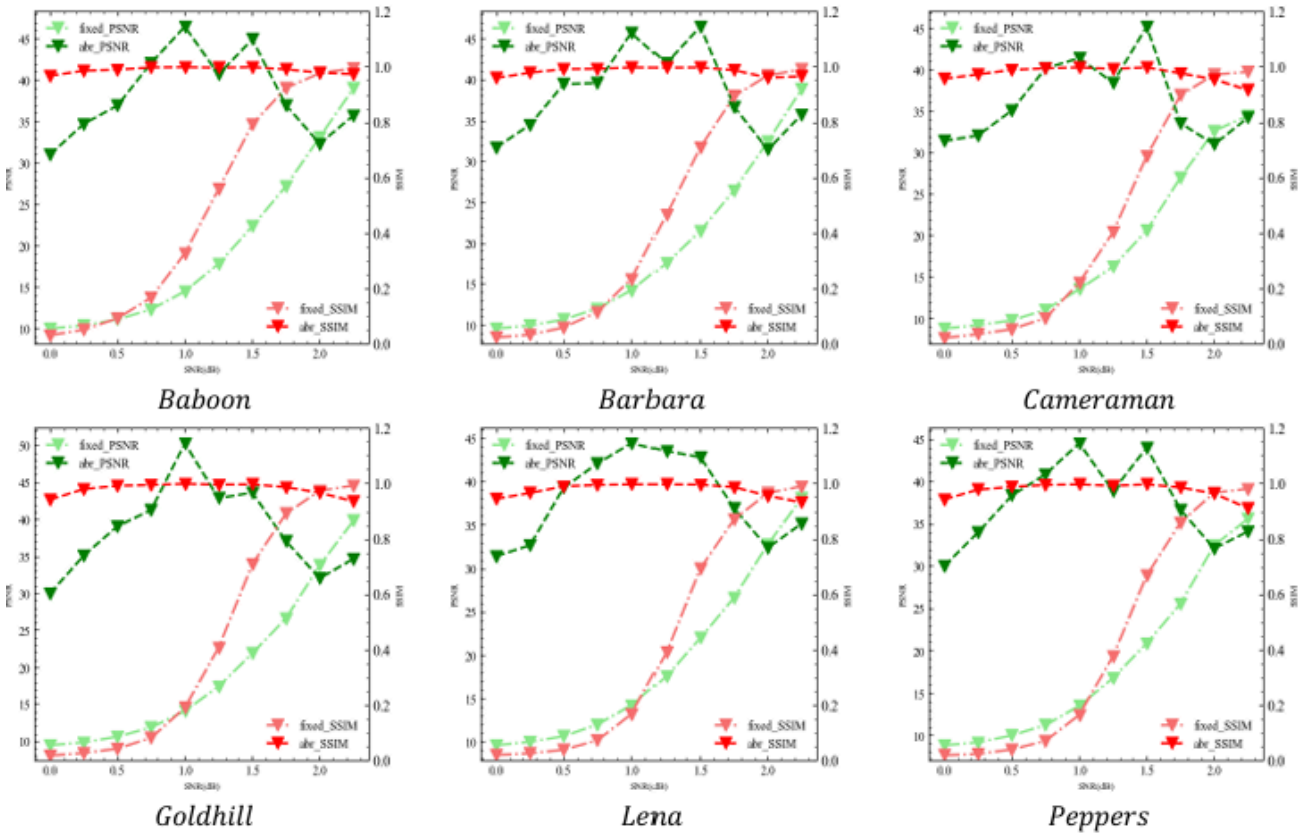


Figure 4. Performance comparison between fixed-rate and variable-rate transmission under different channel conditions

Table 3. Average objective quality metrics under different snr conditions in awgn channels

Image	Metric	Fixed Code Rate	Adaptive Code Rate
Lena	PSNR(dB)	25.23	42.89
	SSIM	0.58	0.95
Baboon	PSNR(dB)	24.92	41.56
	SSIM	0.55	0.99
Barbara	PSNR(dB)	24.78	42.34
	SSIM	0.56	0.93
Cameraman	PSNR(dB)	24.55	43.11
	SSIM	0.54	0.92
Goldhill	PSNR(dB)	24.81	43.57
	SSIM	0.57	0.94
Peppers	PSNR(dB)	25.46	41.54
	SSIM	0.58	0.95

Additionally, Figure 5 illustrates the subjective image quality of Lena transmitted over a low signal-to-noise ratio (SNR = 1.0 dB) AWGN channel using fixed-rate polar codes and the proposed adaptive-rate system. The right side shows the image received by the proposed system, while the left

DOI: 10.54254/2753-8818/2025.GL26091

side shows the image received using fixed-rate coding. It is evident that under low SNR channel conditions, the image visual quality is significantly improved when using the proposed adaptive-rate polar coding system.

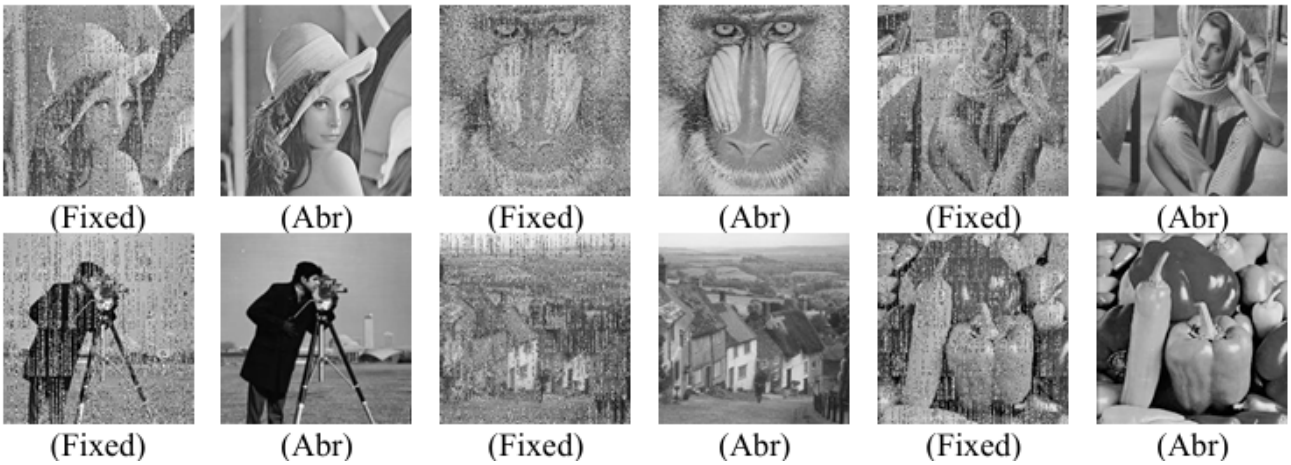


Figure 5. Subjective quality of reconstructed images under awgn channel

5. Conclusion

This paper presents an image transmission system based on adaptive polar codes. By designing a rate lookup table tailored to specific channel conditions, the system can autonomously select coding rate parameters according to channel state information for efficient encoding and decoding. Furthermore, a comprehensive system performance evaluation framework was established, assessing metrics such as bit error rate (BER), peak signal-to-noise ratio (PSNR), and structural similarity index (SSIM). Extensive simulations under various channel conditions verified the advantages of the adaptive polar code over traditional polar coding schemes. Future research can proceed in two directions: Algorithm optimization: Develop more advanced adaptive algorithms that incorporate practical channel factors such as multipath effects, establish precise channel models, and optimize coding parameters to enhance system performance under complex channel conditions. Hardware implementation: Develop dedicated hardware platforms, optimize architectures to improve processing speed and stability, efficiently realize adaptive polar encoding and decoding, reduce power consumption and costs, and enhance device compatibility.

References

[1] Zeng, X. B., et al. (2024). Robust image hiding network with frequency and spatial attentions. Pattern Recognition, 155, 110691.
[2] Huang, J. H., et al. (2025). D 2-JSCC: Digital deep joint source-channel coding for semantic communications. IEEE Journal on Selected Areas in Communications.
[3] Gündüz, D., et al. (2024). Joint source–channel coding: Fundamentals and recent progress in practical designs. Proceedings of the IEEE.
[4] Rowshan, M., et al. (2024). Channel coding towards 6G: Technical overview and outlook. IEEE Open Journal of the Communications Society.
[5] Arikan, E. (2009). Channel polarization: A method for constructing capacity-achieving codes for symmetric binary-input memoryless channels. IEEE Transactions on Information Theory, 55(7), 3051–3073.
[6] Shen, Y. F., et al. (2022). Fast iterative soft-output list decoding of polar codes. IEEE Transactions on Signal Processing, 70, 1361–1376.

DOI: 10.54254/2753-8818/2025.GL26091

[7] Kumari, A., & Kumar, S. (2024). Compressed sensing image communication in Rayleigh fading channel using polar code. Microwave Review, 30(2).
[8] Dong, Y. F., et al. (2021). Joint source and channel coding using double polar codes. IEEE Communications Letters, 25(9), 2810–2814.
[9] Fujihashi, T., et al. (2021). HoloCast+: Hybrid digital-analog transmission for graceful point cloud delivery with graph Fourier transform. IEEE Transactions on Multimedia, 24, 2179–2191.
[10] Yang, J. D., & Liu, Y. (2022). Survey on decoding schemes of the polar code using the deep learning. In International Conference in Communications, Signal Processing, and Systems. Singapore: Springer Nature Singapore.
[11] Wang, Z., Bovik, A. C., Sheikh, H. R., & Simoncelli, E. P. (2004). Image quality assessment: From error visibility to structural similarity. IEEE Transactions on Image Processing, 13(4), 600–612. https: //doi.org/10.1109/TIP.2003.819861